Accepted Manuscript

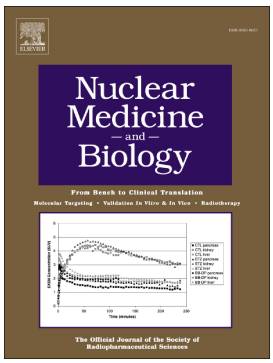

Deuterated 18F-9-O-hexadeutero-3-fluoropropoxyl-(+)-dihydrotetrabenazine (D6-FP-(+)-DTBZ): a vesicular monoamine transporter 2 (VMAT2) imaging agent

Futao Liu, Seok Rye Choi, Zhihao Zha, Karl Ploessl, Lin Zhu, Hank F. Kung

PII: S0969-8051(17)30282-2
DOI: doi:10.1016/j.nucmedbio.2017.11.009
Reference: NMB 7982

To appear in:

Received date: 11 September 2017
Revised date: 21 November 2017
Accepted date: 28 November 2017

Please cite this article as: Futao Liu, Seok Rye Choi, Zhihao Zha, Karl Ploessl, Lin Zhu, Hank F. Kung , Deuterated 18F-9-O-hexadeutero-3-fluoropropoxyl-(+)-dihydrotetrabenazine (D6-FP-(+)-DTBZ): a vesicular monoamine transporter 2 (VMAT2) imaging agent. The address for the corresponding author was captured as affiliation for all authors. Please check if appropriate. Nmb(2017), doi:10.1016/j.nucmedbio.2017.11.009

Deuterated ^{18}F-9-O-hexadeutero-3-fluoropropoxyl-(+)-dihydrotetrabenazine (D6-FP-(+)-DTBZ): a vesicular monoamine transporter 2 (VMAT2) imaging agent

Futao Liu[a,b], Seok Rye Choi[b,c], Zhihao Zha[b], Karl Ploessl[b,c], Lin Zhu[a,b] and Hank F. Kung[b,c] *

[a] Key Laboratory of Radiopharmaceuticals, Beijing Normal University, Ministry of Education, Beijing, 100875, P. R. China

[b] Department of Radiology, University of Pennsylvania, Philadelphia, PA 19104, USA

[c] Five Eleven Pharma Inc., Philadelphia, PA 19104, USA

Re-submitted to Nuclear Medicine and Biology NUCMEDBIO_2017_206R2

Total pages: 35, Word count: 6206, Schemes: 2, Figures: 7, Tables: 4

*Corresponding author contact information:

Hank F. Kung, Ph.D. Department of Radiology, University of Pennsylvania, 3700 Market Street, Room 305, Philadelphia, PA 19104, USA Tel: +1 215 662 3989; Fax: +1 215 349 5035; E-mail: kunghf@sunmac.spect.upenn.edu (H.F. Kung)

Abstract

Introduction: Vesicular monoamine transporters 2 (VMAT2) in the brain serve as transporter for packaging monoamine in vesicles for normal CNS neurotransmission. Several VMAT2 imaging agents, [^{11}C]-(+)-DTBZ, dihydrotetrabenazine and [^{18}F]FP-(+)-DTBZ (9-O-fluoropropyl-(+)-dihydro tetrabenazine, a.k.a. [^{18}F]AV-133), are useful for studying the changes in brain function related to monoamine transmission by in vivo imaging. Deuterated analogs have been reported targeting VMAT2 binding sites.

Methods: A novel deuterated [^{18}F]9-O-hexaduterofluoropropyl-(+)-dihydrotetrabenazine, [^{18}F]D6-FP-(+)-DTBZ, [^{18}F]**1**, was prepared as a VMAT2 imaging agent. This ^{18}F agent which targeted VMAT2 was evaluated by in vitro binding, in vivo biodistribution and microPET imaging studies in rodents.

Results: The one step radiolabeling reaction led to the desired [^{18}F]D6-FP-(+)-DTBZ, [^{18}F]**1**, which showed excellent binding affinity to VMAT2 (Ki = 0.32 ± 0.07 nM) comparable to that of FP-(+)-DTBZ (Ki = 0.33 ± 0.02 nM) using [^{18}F]FP-(+)-DTBZ and rat striatum membrane homogenates. In vivo biodistribution in normal rats showed that **1**, exhibited excellent brain uptake and comparable high ratio of striatum to cerebellum (target/background) ratio at 1 hr after injection (ratio of 6.05 ± 0.43 vs 5.66 ± 0.72 for [^{18}F]FP-(+)-DTBZ vs [^{18}F]**1**, respectively). MicroPET imaging studies in rats further confirm that the striatum with high VMAT2 concentration was clearly delineated in normal rat brain after iv injection of [^{18}F]**1**. We observed minor changes of metabolism in rat plasma between these two agents; however, the changes showed little effect on regional brain uptake and retention.

Conclusions: The results reported here lend support for using [^{18}F]D6-FP-(+)-DTBZ, [^{18}F]**1**, as in vivo PET imaging agent for VMAT2 binding in the brain.

Keywords: monoamine transporter, ^{18}F, deuterium, brain, PET imaging agent, in vivo metabolism

1. Introduction

Hydrogen to deuterium substitution is a novel strategy developing new drugs. Deuterium (D) is a stable isotope of hydrogen (H), which contains one proton and one neutron in the nucleus whereas hydrogen has no neutron. The physical and chemical properties between hydrogen and deuterium are relatively small [1]. Replacement of the carbon hydrogen bond (C-H) with a carbon-deuterium (C-D) bond is known to increase in vivo metabolic stability through a reduction in drug metabolism. Cytochrome P450 enzymes catalyze most of the oxidative reactions that break C-H bonds, such as reactions for O-demethylation or N-demethylation [2, 3], a common step in drug clearance. There are three-value added hydrogen to deuterium substitution that should be described: 1) slows normal in vivo metabolism, allowing for better uptake and retention; 2) slows metabolic side products in vivo reducing un-wanted metabolites; 3) reduces unwanted side reactions in chemical synthesis.

Recent reports on deuterium substituted active pharmaceuticals have indeed demonstrated substantial benefits of the deuterium isotope's kinetic effects on the safety and clearance of drug substances, leading to the creation of new drugs through deuterated versions of existing molecules [4].

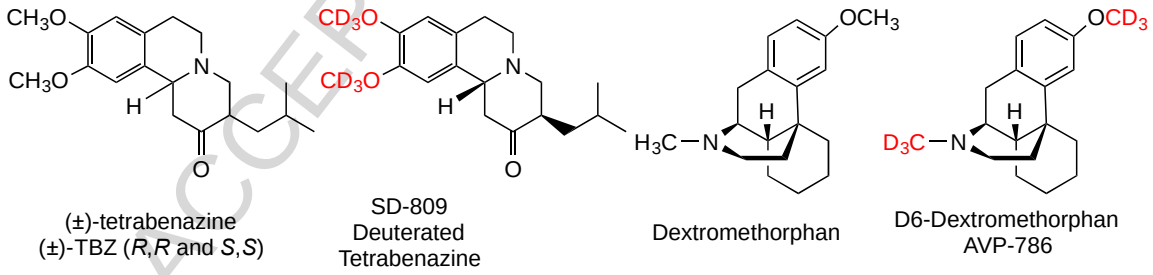

Figure 1. Chemical structures of tetrabenazine ((±)-TBZ, Nitoman or Xenazine) and deuterated tetrabenazine (SD-809, Austedo) and dextromethorphan and D6-dextromethorphan (AVP-786).

The FDA has recently approved tetrabenazine-D6 and D6-dextromethorphan (AVP-786) for treatment of Huntington's and Alzheimer's

disease, respectively (Figure 1). Clinical studies have suggested that SD-809 (tetrabenazine-D6, Austedo) is an analog of tetrabenazine with a slower CYP2D6 metabolism that increases the active drug's in vivo half-life (Figure 1). Prolonged in vivo residence leads to stable dosage exposure that can improve motor activity in patients with Huntington's disease [5, 6]. Deuterated tetrabenazine (SD-809) was approved for treatment of chorea associated with Huntington's disease, while AVP-786, deuterated dextromethorphan, is designed to treat agitation in patients with Alzheimer's disease [7]. By substituting a single methyl group with a deuterated methyl group, the bioisosteric agent, D6-dextromethorphan, provides improved drug efficacy [1]. The ability to moderate drug metabolism through hydrogen to deuterium substitutions then provides a novel approach to solving common complications of imaging agents [2, 8]. The main purpose of substituting deuterium for hydrogen is to slow down the in vivo metabolism to reduce the loss of radioactive tracer targeting a specific enzyme or receptor binding site. One excellent example is the use of [^{11}C]L-deprenyl-D2 (instead of [^{11}C]L-deprenyl) for mapping MAO-B enzyme (monoamine oxidase-B; amine oxygen oxidoreductase-B) activity in the brain [9, 10]. The deuterated tracer is now the preferred agent for mapping MAO-B distribution in the human brain [9, 10].

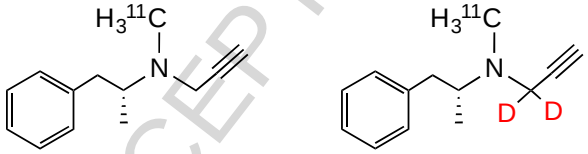

Figure 2. Chemical structures of monoamine oxidase-B (MAO-B), ^{11}C-L-Deprenyl and ^{11}C-L-Deprenyl-D2.

Similarly, a deuterated DTBZ derivative, [^{18}F]fluoroethyl-DTBZ (FE-DTBZ) and the corresponding deuterated [^{18}F]fluoroethyl-DTBZ-D4 ([^{18}F]FE-DTBZ-D4) (Figure 1), [11, 12] have been prepared for imaging VMAT2 in the pancreas. While specific binding to the pancreas did not improve, the in vivo metabolism of

the deuterated [^{18}F]FE-DTBZ-D4 showed a slower washout rate in the blood, suggesting that deuterated probes may prolong plasma resident time.

Dihydrotetrabenazine ([^{11}C]-(+)-DTBZ) and fluoroalkyl derivatives of dihydro-tetrabenazine, [^{18}F]FP-(+)-DTBZ, a.k.a. AV-133 (Figure 3) have been successfully evaluated as imaging agents for vesicular monoamine transporter 2 (VMAT2) in the brain [13, 14]. The ^{18}F labeled fluoropropyl-(+)-dihydrotetrabenazine ([^{18}F]FP-(+)-DTBZ, [^{18}F]AV-133) (Figure 3), with a longer physical half-life than ^{11}C ($T_{1/2}$ = 110 min vs 20 min), has also been developed [13]. In the past few years many reports have appeared in the literature describing the clinical usefulness of [^{18}F]AV-133 as a VMAT2 imaging agent. Results of human clinical studies for [^{18}F]AV-133/PET have suggested that it is a very useful agent in assisting diagnosis and monitoring of Parkinson's disease [15-20].

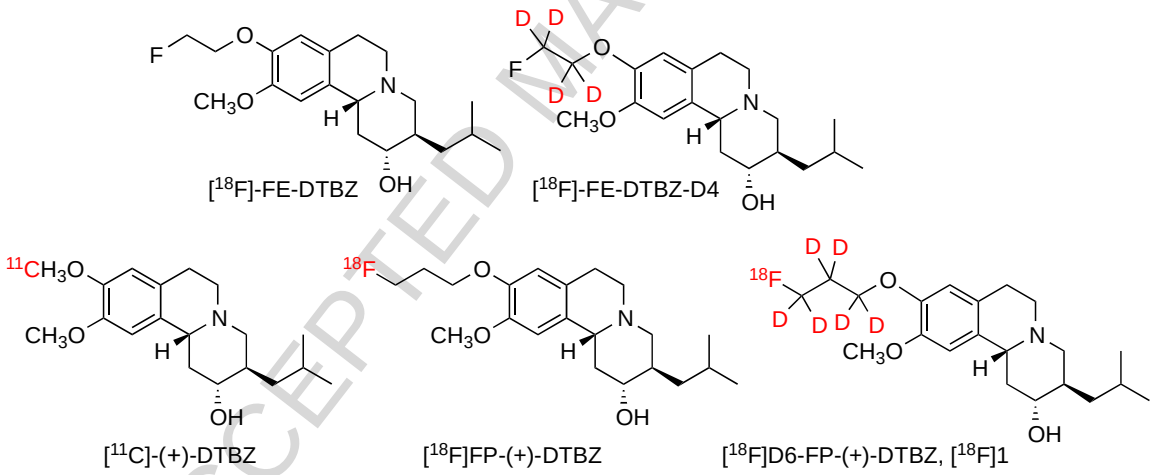

Figure 3. Chemical structures of [^{11}C]-(+)-DTBZ and [^{18}F]FP-(+)-DTBZ (^{18}F-fluoropropyl-(+)-dihydrotetrabenazine) are shown. Both ligands have been tested in humans as vesicular monoamine transporter 2 (VMAT2) imaging agents for diagnosis of Parkinson's disease and β-cells in pancreas [21, 22]. [15, 17, 23-25], targeting VMAT2 binding sites, have been successfully developed and applied for studying patients with Parkinson disease and other movement disorders. [26].

By hydrogen to deuterium substitution, a new deuterated [^{18}F]FP-(+)-DTBZ, namely, [^{18}F]D6-FP-(+)-DTBZ, [^{18}F]**1**, was prepared and tested. In the report herein are the results demonstrating that the deuterium substitution leads to an excellent imaging agent, [^{18}F]D6-FP-(+)-DTBZ, [^{18}F]**1**, (Figure 3) targeting VMAT2 binding sites in the brain.

2. Materials and Methods

2.1 General

All reagents and solvents were commercial products, purchased from Aldrich, Acros, Alfa and Fisher, and were used without further purification, unless otherwise indicated. Solvents were dried through a molecular sieve system (Pure Solve Solvent Purification System; Innovative Technology, Inc.).^{1}H spectra and ^{13}C NMR were recorded on an Avance spectrometer at 400 and 100 MHz, respectively, and referenced to NMR solvents as indicated. Chemical shifts are reported in units of ppm (δ), with a coupling constant, *J*, in Hz. Multiplicity is defined by singlet (s), doublet (d), triplet (t), broad (br), and multiplet (m). High-resolution mass spectrometry (HRMS) data was obtained with an Agilent (Santa Clara, CA) G3250AA LC/MSD TOF system. Thin-layer chromatography (TLC) analyses were performed using Merck (Darmstadt, Germany) silica gel 60 F 254plates. Generally, crude compounds were purified by flash column chromatography (FC) packed with silica gel (Aldrich).

2.2 Synthesis of Compound D6-FP-(+)-DTBZ, 1. (scheme 1)

Scheme 1

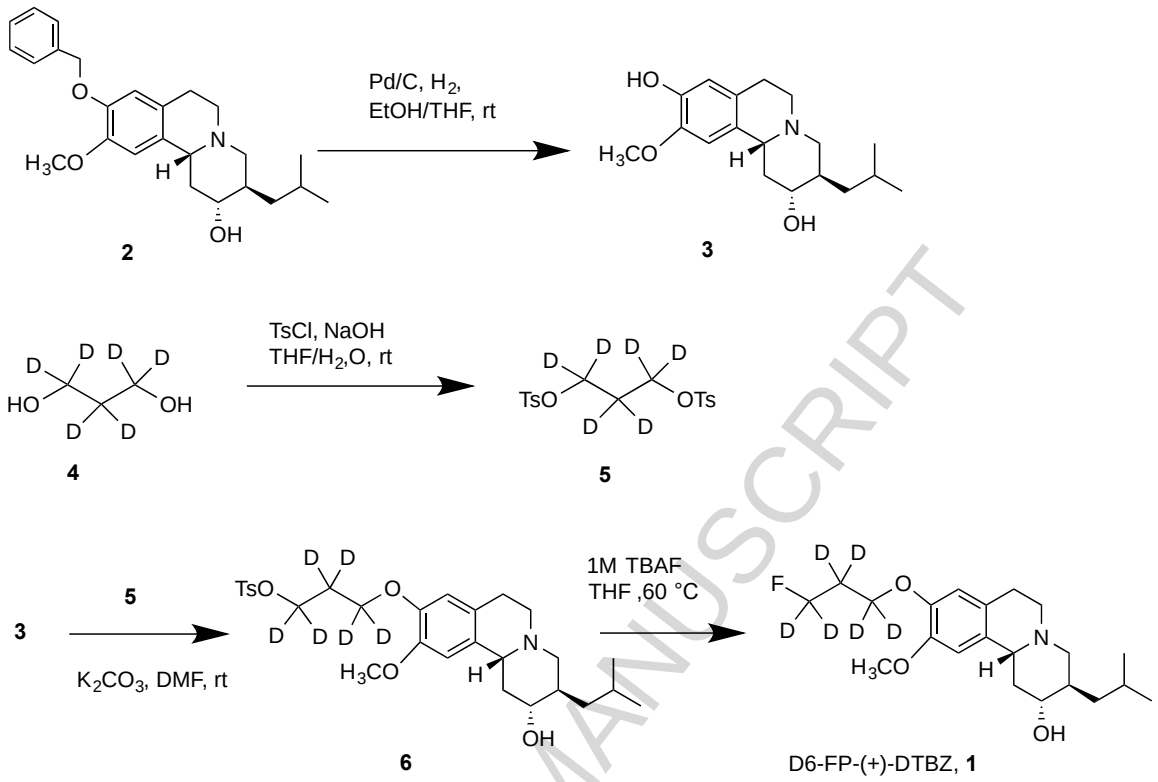

*2.3. Synthesis of compound **3**: (2R,3R,11R)-3-Isobutyl-10-methoxy-2,3,4,6,7,11b-hexahydro-1H-pyrido[2,1-a]isoquinoline-2,9-diol*

A mixture of 9-benzyl protected DTBZ compound **2** (380 mg, 0.96 mmol) and 10% dry Pd/C (15 mg) was stirred in THF (10 mL) and EtOH (5 mL) under H_2 at room temperature for 6 h. The reaction mixture was filtered and washed with EtOH (10 mL) and THF (10 mL). The solvent was removed under vacuum to give compound **3** (255 mg, 87%) as a yellow solid. ^{1}HNMR (400 MHz, $CDCl_3$) δ 6.68 (s, 1 H), 6.67 (s, 1 H), 3.87 (s, 3H), 3.44 - 3.38 (m, 1H), 3.16 - 2.97 (m, 4 H), 2.66 - 2.56 (m, 2 H), 2.49- 2.42 (m, 1 H), 1.99 (t, *J* = 2.01 Hz, 1 H), 1.79 - 1.68 (m, 2 H), 1.57 - 1.45 (m, 3 H), 1.12 - 1.05 (m, 1 H), 0.97 - 0.93 (m, 6 H). HRMS calcd. for $C_{18}H_{27}NO_3$ $[M+H]^+$ 306.2069. found 306.2100.

*2.4. Synthesis of compound **5**: [1,1,2,2,3,3-D_6]-Propane-1,3-diylbis(4-methylbenzenesulfonate)*

To a solution of compound 4 (270 mg, 3.29 mmol) (99 atom %D) in THF (10 mL) was added NaOH (527 mg, 13.17 mmol) in H_2O (5 mL) at 0°C. The reaction mixture was stirred at room temperature for 1 h. TsCl (1.88 g, 9.88 mmol) in THF (10 mL) was then added dropwise. The reaction was stirred at room temperature for 24 h. Water (20 mL) was added and the mixture was extracted with ethyl acetate (3 × 30 mL). The organic layers were combined and dried over anhydrous $MgSO_4$, filtered and the filtrate was evaporated in vacuum, purified by flash chromatography (silica gel) (ethyl acetate (EA)/hexanes, 0% to 60%, vol/vol) to give [1,1,2,2,3,3-D6]-propane-1,3-diylbis(4-methylbenzenesulfonate), compound **5**, (970 mg, 76%) as a white solid. ^{1}HNMR (400 MHz, $CDCl_3$) δ 7.78 - 7.76 (m, 4 H), 7.38 - 7.36 (m, 4 H), 2.483 (s, 6 H), HRMS calcd. for $C_{17}H_{14}D_6O_6S_2$ $[M+H]^+$ 391.1156. found 391.1140.

*2.5. Synthesis of compound **6**: 3-(((2R,3R,11R)-2-Hydroxy-3-isobutyl-10-methoxy-2,3,4,6,7,11b-hexahydro-1H-pyrido[2,1-a]isoquinolin-9-yl)oxy)propyl-[1,1,2,2,3,3-D_6])-4-methylbenzenesulfonate.*

A mixture of compound **3** (44 mg, 0.14 mmol) and K_2CO_3 (119 mg, 0.86 mmol) was stirred in DMF (4 mL) at room temperature for 1 h. Compound **5** (68 mg, 0.17 mmol) was then added and the reaction mixture was stirred for 24 h at room temperature. Water (5 mL) was added, and the mixture was extracted with ethyl acetate (5 × 15 mL). The organic layers were combined and dried over anhydrous $MgSO_4$, filtered and the filtrate was evaporated in vacuum, purified by flash chromatography (silica gel) (MeOH/DCM, 0% to 10%, vol/vol) to give compound **6** (49 mg, 65%) as a light yellow solid. ^{1}HNMR (400 MHz, $CDCl_3$) δ 7.80 - 7.78 (m, 2 H), 7.30 - 7.29 (m, 2 H), 6.68 (s, 1 H), 6.54 (s, 1H), 3.78 (s, 3 H), 3.43 - 3.39 (m, 1H), 3.15 - 2.97 (m, 4 H), 2.65 - 2.57 (m, 2 H), 2.50 - 2.44 (m, 1 H), 2.43 (s, 3H), 2.00 (t, J = 2.01 Hz, 1H), 1.78 - 1.68 (m, 2 H), 1.64 - 1.47 (m, 3 H), 1.12 - 1.05 (m, 1 H), 0.98 - 0.94 (m, 6 H). ^{13}C NMR (100 MHz, $CDCl_3$) δ

147.74, 146.52, 144.68, 132.97, 130.15, 129,78, 127,81, 126,55, 113.89, 108.75, 74.43, 60.91, 60.06, 56.06, 51.84, 41.50, 40.49, 39.67, 29.04, 25.33, 24.13, 21.77, 21.61. HRMS calcd. for $C_{28}H_{33}D_6NO_6S$ $[M+H]^+$ 524.2953. found 524.2963.

*2.6. Synthesis of compound D6-FP-(+)-DTBZ, **1**: (2R,3R,11R)-9-(3-Fluoropro-poxy-[1,1,2,2,3,3-D_6])-3-isobutyl-10-methoxy-2,3,4,6,7,11b-hexahydro-1H-pyrido [2,1-a]isoquinolin-2-ol.*

A mixture of compound **6** (30 mg, 0.06 mmol) and 1M TBAF in THF (0.17 mL, 0.17 mmol) was stirred in anhydrous THF (5 mL) at 60°C for 5 h. H_2O (5 mL) was added, and the mixture was extracted with ethyl acetate (5 × 10 mL). The organic layers were combined and dried over anhydrous $MgSO_4$, filtered and the filtrate was evaporated in vacuum, purified by flash chromatography (silica gel) (MeOH/DCM, 0% to 10%, vol/vol) to give D6-FP-(+)-DTBZ, 1 (16 mg, 75%) as a light yellow solid. ^{1}HNMR (400 MHz, $CDCl_3$) δ 6.71 (s, 1 H), 6.64 (s, 1 H), 3.84 (s, 3H), 3.44 - 3.38 (m, 1 H), 3.16 - 2.98 (m, 4 H), 2.66 - 2.57 (m, 2 H), 2.51 - 2.44 (m, 1 H), 2.00 (t, *J* = 2.01 Hz, 1 H), 1.79 - 1.68 (m, 2 H), 1.56 - 1.47 (m, 3 H), 1.12 - 1.05 (m, 1 H), 0.97 - 0.94 (m, 6 H). ^{13}C NMR (100 MHz, $CDCl_3$) δ 147.80, 146.80, 130.00, 126.61, 113.79, 108.76, 74.58, 60.91, 60.08, 56.15, 51.88, 41.62, 40.55, 39.70, 29.10, 25.36, 24.12, 21.78. HRMS calcd. for $C_{21}H_{26}D_6FNO_3$ $[M+H]^+$ 372.2821. found 372.2824.

2.7. Synthesis of Compound [^{18}F]D6-FP-(+)-DTBZ, [^{18}F]1. (scheme 2)

Scheme 2

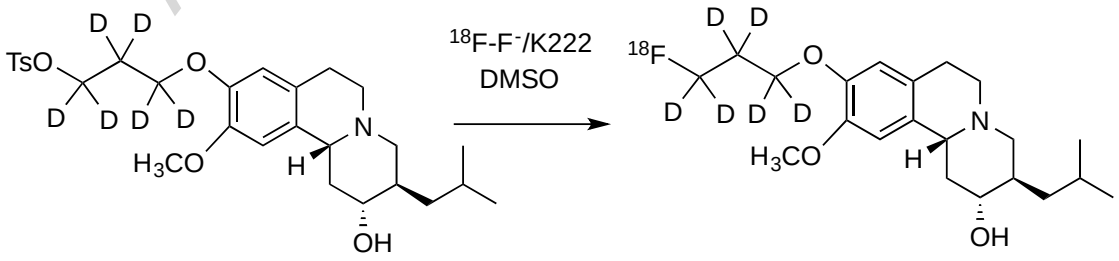

6 [^{18}F]D6-FP-(+)-DTBZ, [^{18}F]**1**

Preparation of [^{18}F]D6-FP-(+)-DTBZ, [^{18}F]**1** by radiolabeling was accomplished by the following steps. ^{18}F fluoride was loaded on an activated QMA light cartridge and eluted with 0.7 mL K_{222}/K_2CO_3 solution (40 mg K_2CO_3, 220 mg K_{222}, 3.6 mL water, 18.4 mL ACN) into conical vial. The solution was dried under a flow of argon at 80 °C and azeotropically dried twice with 1 mL acetonitrile. 1 mg compound **6** was dissolved in 0.5 ml DMSO (anhydrous) and added to dried [^{18}F]$F^-/K_{222}/K_2CO_3$ complex. The reaction mixture was heated for 15 min at 115 ºC. The resulting reaction mixture was cooled to room temperature and added to 8 mL water. The mixture was loaded onto an Oasis HLB (3cc) cartridge. Eluted and washed twice with 3 mL water. The desired [^{18}F]D6-FP-(+)-DTBZ was eluted with 1 ml acetonitrile. To this solution was added about 1 mL of 10 mM AFB and injected onto semiprep HPLC (Phenomenex Gemini 250 ×10 mm, ACN/10 mM AFB 45/55, 3 mL/min). The fraction of the desired **[^{18}F]1** was collected (retention time 14 – 15 min). The solution was mixed with 14 mL water and added onto an Oasis HLB 3cc. After elution, the SPE was washed with 3 mL water. The activity was eluted with 1 mL 100% ethanol. Solution was concentrated to about 200 µL volume and diluted with 1.8 mL saline buffer. HPLC profile on HPLC (HPLC: Supelco Ascentis 150 × 4.6 mm, ACN/10 mM AFB 45/55, 1 mL/min) showed single peak at 6 minutes for [^{18}F]**1.** The retention time corresponded to the nonradioactive standard D6-FP-(+)-DTBZ, **1.**

The corresponding non-deuterated [^{18}F]FP-(+)-DTBZ was prepared similarly as described above.

2.8. In vitro binding assay for Ki determination

Tissue homogenates of striatum (dissected from rat brain) were prepared in 50 mM of HEPES, pH 7.5, and 0.3 M of sucrose. Compounds were examined for their ability to compete for the binding of [^{18}F]FP-(+)-DTBZ or [^{18}F]D6-FP-(+)-DTBZ (0.15 - 0.2 nM) at concentrations ranging from 10^{-7} to 10^{-12} M. The binding assays were performed in glass tubes (12 x 75 mm) in a final volume of 0.25 mL. The nonspecific binding was defined with 10 µM (±)-tetrabenazine (TBZ). After

incubation for 90 min at room temperature, the bound ligand was separated from the free ligand by filtration through glass fiber filters. The filters were washed three times with 4 mL of ice-cold PBS buffer, pH 7.4 and the radioactivity on the filters was counted with a gamma counter (WIZARD^2, Perkin-Elmer). Data were analyzed using the nonlinear least-square curve fitting program LIGAND to determine IC_{50} and Ki was calculated by Cheng-Prusoff equation using 0.11 nM as Kd of [^{18}F]FP-(+)-DTBZ and [^{18}F]D6-FP-(+)-DTBZ.

2.9. In vivo biodistribution in rats

Three rats per group were used for each biodistribution study. While under isoflurane anesthesia, 0.2 mL of a saline solution containing 20 µCi of radioactive tracer, [^{18}F]FP-(+)-DTBZ or [^{18}F]D6-FP-(+)-DTBZ, was injected into the femoral vein. The rats were sacrificed at the time indicated by cardiac excision while under isoflurane anesthesia. Organs of interest were removed and weighed, and the radioactivity was counted. Different regions of brain (cortex, striatum, hippocampus, cerebellum and hypothalamus) were dissected, weighed and counted. The percent dose per organ was calculated by comparing the tissue counts to counts of 1% of the initial dose (100 times diluted aliquots of the injected material) measured at the same time. The ratio was calculated by dividing the percentage dose/g of each region by that of the cerebellum. The cerebellum was used as the reference region for calculating the ratio of target to non-target binding, because only a trace amount of VMAT2 binding site is present in the cerebellum.

2.10. Ex vivo autoradiography

A normal CD-1 mouse was injected with 0.7 mCi [^{18}F]D6-FP-(+)-DTBZ and sacrificed at 30 min post-injection. The brain was harvested and frozen. 20 µm thick coronal sections were cut on a cryostat, thaw mounted onto slides and dried at room temperature. The dried sections were exposed to imaging plate for

30 min and images were acquired using the Typhoon FLA 7000 (GE Healthcare Life Sciences).

2.11. MicroPET imaging in rats

Dynamic microPET imaging of rat brain was performed using Philips Mosaic Animal PET (A-PET) imaging system. Two tracers were imaged in the same rat. Rat was anesthetized with 1.5% isoflurane in oxygen, positioned on the bed of the microPET gantry, and fixed near the center of the scanner. Isoflurane anesthesia was continued throughout the study. Rat was injected intravenously via the tail vein with 0.96 mCi of [^{18}F]FP-(+)-DTBZ and with 0.92 mCi of [^{18}F]D6-FP-(+)-DTBZ on the next day. The scan duration was 120 min from the time of injection. Scans were obtained in the frame sequence of 5 min. The data were histogrammed into 24 consecutive frames, and the images were reconstructed. Images were analyzed with AMIDE (http://amide.sourceforge.net/). Frames were summed to manually draw regions of interest (ROIs). ROIs were drawn manually from two brain regions (striatum and cerebellum), and time–activity curves for the ROIs were obtained. The size of the gantry and the field of view were not suitable for a whole rat imaging; therefore additional microPET imaging studies, which allowed the imaging examining of spine (bone uptake), were carried out and described below.

Whole-body PET images of rats were obtained using a β-cube (Molecubes, Belgium). The same rat was imaged with two tracers. Rat was injected intravenously via the tail vein with 0.47 mCi of [^{18}F]FP-(+)-DTBZ and with 0.50 mCi of [^{18}F]D6-FP-(+)-DTBZ on the next day. The scan duration was 10 min at 60 min post- injection.

2.12. In vivo metabolism study in mice and rats

Mice and rats were anesthesized with 1.5% isoflurane in oxygen. The animals were injected with 1 – 2 mCi of [^{18}F]D6-FP-(+)-DTBZ or [^{18}F]FP-(+)-DTBZ (0.1 - 0.2 mL, 10% ethanol in saline). The animals were then sacrificed at

30 or 60 min after the intravenous injection. Blood, brain and liver were harvested. Blood samples were centrifuged at 15,000*g* for 2 min at 4 °C to separate plasma from the clot. Plasma was then collected and the same volume of CH_3CN was added and the resulting mixture was vortexed and centrifuged at 15,000*g* for 2 min for deproteinization. Brain and liver were homogenized in a solution of ice-cooled PBS and the same volume of CH_3CN was added. Homogenates were then centrifuged at 15,000*g* for 2 min at 4 °C and the supernatant was collected. An aliquot of the supernatant obtained from plasma, liver or brain homogenate was injected into the radio-HPLC system, and analyzed under the analytical conditions (column: Phenomenex Luna 5 micron C18 150 × 46 mm, flow rate: 1 mL/min, solvent: 80% 0.1 N ammonium formate pH 4.1: 20% acetonitrile). The percentages of [^{18}F]D6-FP-(+)-DTBZ relative to total radioactivity (corrected for decay) on HPLC were calculated as (peak area for unchanged tracer peak/total peak area) × 100. The same samples also were analyzed with TLC (Silica 254F plate with the developing solvent of chloroform/ethanol/ammonium hydroxide = 8/2/drop).

3. Results and Discussion

Both ligands, the deuterated [^{18}F]D6-FP-(+)-DTBZ and the non-deuterated [^{18}F]FP-(+)-DTBZ, were successfully radiolabeled with excellent labeling yields and high chemical purity after HPLC purification ([^{18}F]D6-FP-(+)-DTBZ**:** length of procedure: ~ 1 hr; activity used: 26.3 ± 7.6 mCi (n = 6); RCY 58.8 ± 5.3% (dc): RCP: 99%; molar activity 482 ± 240 Ci/mmol (measured at 280 nm)) ([^{18}F]FP-(+)-DTBZ: length of procedure: ~ 1 hr; activity used: 21.9 ± 8.1 mCi (n = 6); RCY 66.8 ± 3.2% (dc): RCP: 99%; molar activity 478 ± 153 Ci/mmol (measured at 280 nm)). The results were similar to that reported previously for [^{18}F]FP-(+)-DTBZ [18].

Using either [^{18}F]D6-FP-(+)-DTBZ or [^{18}F]FP-(+)-DTBZ as the hot ligand and homogenates of striatum (dissected from rat brain), binding affinities of (±)-TBZ, FP-(+)-DTBZ and D6-FP-(+)-DTBZ were measured. Results (Table 1)

suggest that the binding affinities of either the deuterated and non-deuterated DTBZ derivative were very similar. Excellent correlation was observed suggesting the deuterium to hydrogen substitution exhibited no negative effect on the in vitro binding affinity.

Table 1. Comparison of in vitro binding affinities (Ki, nM of (±)-TBZ, FP-(+)-DTBZ, and D6-FP-(+)-DTBZ) to vesicular monoamine transporter 2 (VMAT2)

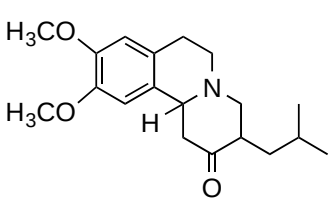

(±)-tetrabenazine
(±)-TBZ (*R*,*R* and *S*,*S*)

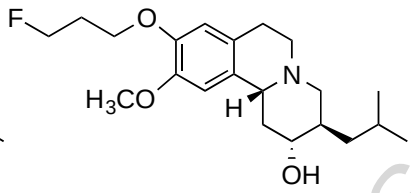

FP-(+)-DTBZ

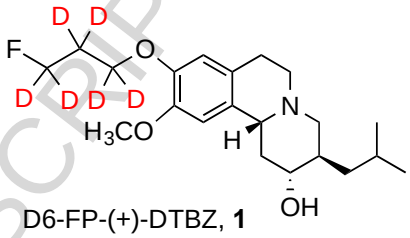

D6-FP-(+)-DTBZ, **1**

Radiotracer	Ki of cold competing drug (nM, Avg ± SD, n = 3)		
	(±)-TBZ	FP-(+)-DTBZ (AV-133)	D6-FP-(+)-DTBZ, **1**
[^{18}F]D6-FP-(+)-DTBZ	1.65 ± 0.07	0.26 ± 0.03	0.33 ± 0.06
[^{18}F]FP-(+)-DTBZ	1.49 ± 0.24	0.33 ± 0.02	0.32 ± 0.07

* In vitro binding studies were performed using rat striatum homogenates

As expected (±)-TBZ showed a lower binding affinity comparable to reported in the literature (Ki = 1.49 or 1.65 nM, depending on the ligand used). The binding affinity of (±)-TBZ reported in Table 1 is similar to that reported previously [13, 27]. Results of binding studies for **[**^{18}F]FP-(+)-DTBZ or [^{18}F]D6-FP-(+)-DTBZ (Ki = 0.26 to 0.33 nM, Table 1) showed that hydrogen to deuterium substitution provided the same binding affinity to the VMAT2 binding sites [27]. There is no difference in binding affinity. The results showed that [^{18}F]D6-FP-(+)-DTBZ is an excellent PET imaging agent for VMAT2 binding sites.

Table 2. Biodistribution in normal male CD IGS rats after an IV injection of [^{18}F]D6-FP-(+)-DTBZ (average of 3 rats ± SD)

% dose/g	2 min	60 min	120 min
Blood	0.23±0.03	0.11±0.01	0.10±0.00
Heart	0.69±0.12	0.26±0.01	0.21±0.01
Muscle	0.17±0.02	0.11±0.00	0.09±0.01
Lung	0.87±0.05	0.49±0.00	0.41±0.01
Kidney	1.89±0.07	0.66±0.04	0.59±0.02
Spleen	1.04±0.10	0.66±0.03	0.51±0.03
Pancreas	2.62±0.15	5.01±0.69	4.49±0.17
Liver	2.79±0.12	3.19±0.46	3.10±0.49
Skin	0.24±0.02	0.25±0.01	0.21±0.01
Brain	0.64±0.07	0.44±0.02	0.34±0.02
Bone	0.33±0.04	0.47±0.02	0.65±0.03

Ratio vs. Cerebellum for [^{18}F]D6-FP-(+)-DTBZ

	2 min	60 min	120 min
Cerebellum	1.00±0.00	1.00±0.00	1.00±0.00
Striatum	2.08±0.30	6.05±0.43	5.49±0.43
Hippocampus	1.26±0.04	1.68±0.12	1.74±0.32
Cortex	1.36±0.05	1.13±0.02	1.10±0.09
Remainder	1.33±0.03	1.59±0.04	1.52±0.03
Hypothalamus	1.71±0.10	3.93±0.15	3.56±0.49

Table 3. Biodistribution in normal male CD IGS rats after an IV injection of [^{18}F]FP-(+)-DTBZ (average of 3 rats ± SD)

% dose/g	2 min	60 min	120 min
Blood	0.24±0.03	0.12±0.00	0.07±0.01
Heart	0.96±0.08	0.22±0.03	0.16±0.01
Muscle	0.11±0.02	0.10±0.01	0.07±0.00
Lung	1.03±0.03	0.41±0.03	0.31±0.02
Kidney	2.66±0.15	0.63±0.05	0.45±0.02
Spleen	1.19±0.10	0.50±0.04	0.37±0.05
Pancreas	2.29±0.36	4.48±0.27	3.56±0.42
Liver	2.28±0.04	2.59±0.21	2.12±0.20
Skin	0.19±0.03	0.24±0.03	0.17±0.01
Brain	0.83±0.06	0.35±0.03	0.26±0.03
Bone	0.45±0.03	1.13±0.07	1.86±0.24

Ratio vs. Cerebellum for ^{18}F-FP-(+)DTBZ

	2 min	60 min	120 min
Cerebellum	1.00±0.00	1.00±0.00	1.00±0.00
Striatum	1.66±0.15	5.66±0.72	6.54±0.59
Hippocampus	1.19±0.03	1.64±0.19	1.79±0.12
Cortex	1.21±0.04	1.13±0.09	1.11±0.09
Remainder	1.23±0.03	1.68±0.07	1.59±0.09
Hypothalamus	1.57±0.04	3.91±0.37	4.04±0.66

Comparison biodistribution study in rats between [^{18}F]D6-FP-(+)-DTBZ and [^{18}F]FP-(+)-DTBZ (Table 2 and 3) demonstrated that there was good similarity. However, the most noticeable difference was the bone uptake. The deuterated **[^{18}F]1** showed a clearly distinctive lowering of the bone uptake, the bone uptake at 60 and 120 min were 1.13 and 1.86% dose/g for [^{18}F]D6-FP-(+)-DTBZ while the deuterated [^{18}F]D6-FP-(+)-DTBZ showed bone uptake of 0.47 and 0.65% dose/g, respectively. The lowering of the bone uptake is likely associated with a higher bond energy of C-D as compared to C-H; as a consequence it reduces the level of free ^{18}F fluoride in the blood circulation.

One other major observation is the improved brain retention at 120 min after iv injection. The total brain uptake were 0.26 vs 0.34% dose/g for [^{18}F]FP-(+)-DTBZ and [^{18}F]D6-FP-(+)-DTBZ respectively. This amounts to a 30% increase in total brain uptake. However, these two agents showed comparable regional brain uptake ratios; at 60 min post i.v. injection the striatum/cerebellum ratios were 5.66 vs 6.05 for [^{18}F]FP-(+)-DTBZ and [^{18}F]D6-FP-(+)-DTBZ respectively.

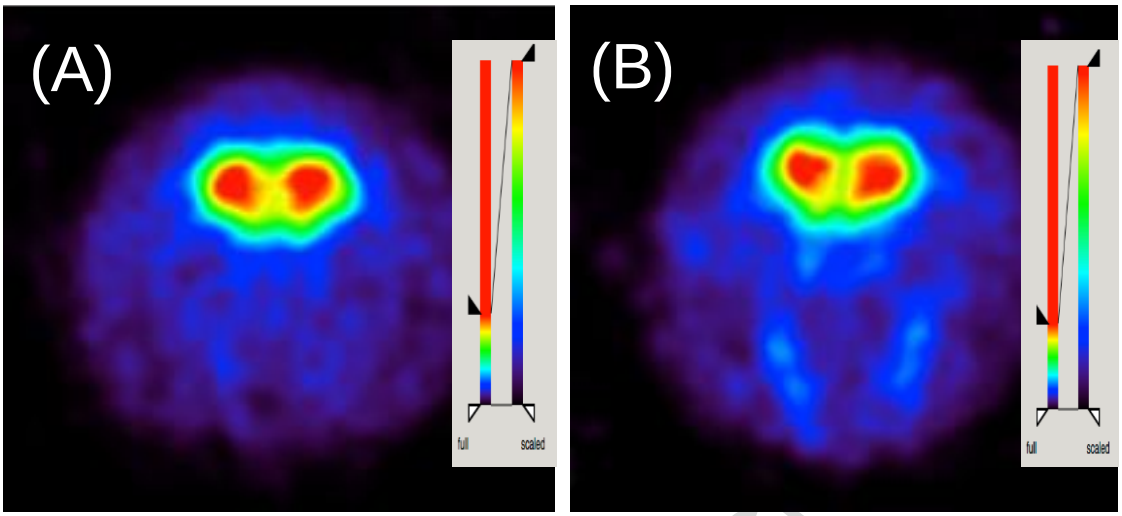

Fig 4. MicroPET images of [^{18}F]D6-FP-(+)-DTBZ (A) and [^{18}F]FP-(+)-DTBZ (B) in the brain of normal rat. Each PET image was generated by the summation of data collected 50 - 60 min after injection.

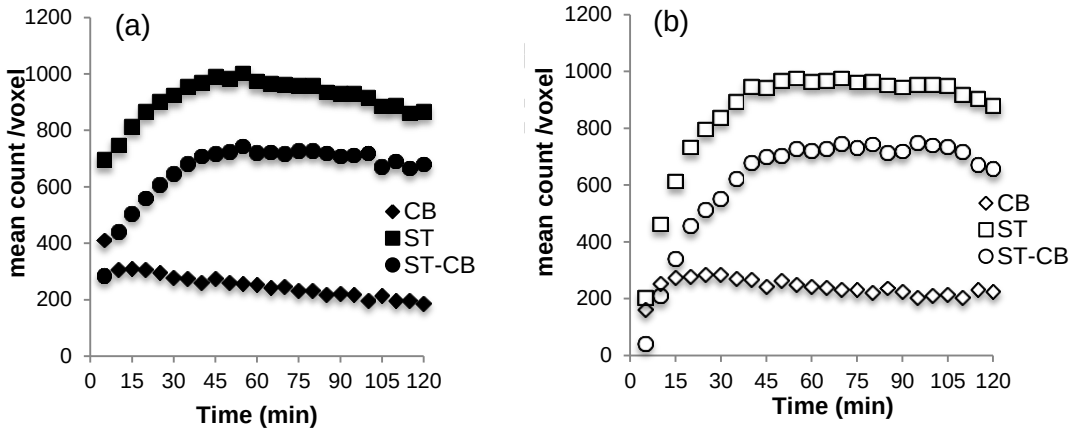

Fig 5. Time–activity curves of [^{18}F]D6-FP-(+)-DTBZ (a) and [^{18}F]FP-(+)-DTBZ (b) in the brains of normal rat, expressed as the mean count/voxel, for striatum (ST) and cerebellum (CB). PET data were collected for 120 min. Regions of interest (ROIs) were identified according to the stereotaxic atlas. The radioactivities in the striatum and cerebellum were plotted against the time post-injection.

[^{18}F]D6-FP-DTBZ and [^{18}F]FP-DTBZ binding to VMAT2 in the brain was compared in vivo by performing microPET imaging in the same rat. Coronal

microPET images of normal rat brains at 0-120 min after tail vein injection of [^{18}F]D6-FP-(+)-DTBZ and [^{18}F]FP-DTBZ are shown in Fig. 4A and 4B, respectively. MicroPET imaging with [^{18}F]D6-FP-(+)-DTBZ in normal rat produced high-quality images, as shown in Fig. 4A. A high accumulation of radioactivity was observed in the striatum, the site with the highest concentrations of VMAT2. These in vivo microPET results confirmed the affinity of [^{18}F]D6-FP-(+)-DTBZ to VMAT2. Figure 5 shows time–radioactivity curves for the striatum and cerebellum following tail vein injection of [^{18}F]D6-FP-(+)-DTBZ. After the injection of [^{18}F]D6-FP-(+)-DTBZ the radioactivity was rapidly taken up by the brain, with the striatum exhibiting maximal activity around 45 min. The clearance of radioactivity from brain regions was also very rapid, with good differentiation of the striatum from the cerebellum visible 10 min after injection. The striatum exhibited the highest uptake level and good retention of the radioligand. The striatum to cerebellum ratios (ST/CB) of radioactivity were 3.84 and 3.48 for [^{18}F]D6-FP-(+)-DTBZ and [^{18}F] FP-DTBZ**.**

In addition to dynamic scans, we performed whole body scans in the same rats with both tracers. Both tracers showed high specific localization in striatum. Furthermore, **[**^{18}F]D6-FP-DTBZ demonstrated much lower bone uptakes compared to that of **[**^{18}F]FP-DTBZ. These results are correlating well with biodistribution data.

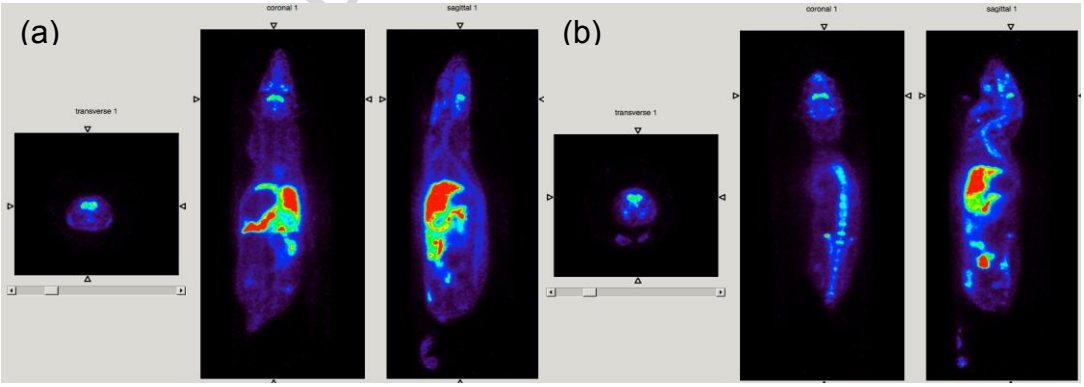

Fig 6. Whole body images of (a) [^{18}F]D6-FP-(+)-DTBZ and (b) [^{18}F]FP-(+)-DTBZ in a normal rat. Each PET image was generated using βCUBE by data collected for 20 min at 60 - 80 min after injection.

As shown in Fig 6, regional distribution of [^{18}F]D6-FP-(+)-DTBZ in the mouse brain was evaluated by ex vivo autoradiography. Autoradiograms of [^{18}F]D6-FP-(+)-DTBZ displayed intense labeling in the caudate putamen, accumbens, substantial nigra, hypothalamic nucleus, dorsal raphe and locus coeruleus reflecting VMAT2 density. The resulting images were well aligned with the animal PET imaging results and regional brain tissue dissection data showing high tracer uptake and retention in regions of brain with high VMAT2 density.

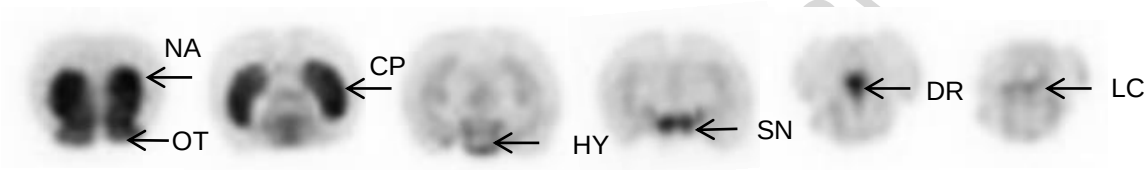

Fig 7. Ex vivo autoradiography of VMAT2 binding sites in a mouse brain. 0.7 mCi of [^{18}F]D6-FP-(+)-DTBZ was injected into a normal CD-1 mouse and sacrificed at 30min post-injection. The intensity of [^{18}F]D6-FP-(+)-DTBZ binding were well matched with the VMAT2 expression in the brain. NA: nucleus accumbens, HY: Hypothalamic nucleus, SN: Substantia nigra, DR: dorsal raphe, LC: locus coeruleus.

Plasma, homogenized brain and liver extracts from rat were examined to evaluate in vivo stability of [^{18}F]D6-FP-(+)-DTBZ and [^{18}F]FP-(+)-DTBZ using radio-HPLC. Table 4 (n = 2) shows the percentages of unchanged [^{18}F]D6-FP-(+)-DTBZ and [^{18}F]FP-(+)-DTBZ in the total radioactivity of plasma, brain liver tissues at 30 or 60 min after radiotracer injection. The recovery of radioactivity into the supernatant was 68-75%, 82-86% and 76-82% for plasma, brain and liver respectively. TLC and HPLC methods detected the same pattern of metabolite formation with both radiotracers. All radiolabeled metabolites were more polar than parent radiotracers. [^{18}F]D6-FP-(+)-DTBZ showed improved plasma stability which agree with the lower bone uptakes of [^{18}F]D6-FP-(+)-DTBZ in rats. In addition, [^{18}F]D6-FP-(+)-DTBZ demonstrated improved metabolic stability in mice brain. However, these results need to be confirmed

further using a larger number of animals and more data points and eventually evaluated in humans. In vitro microsomal metabolism studies to characterized the metabolites using LC-MS are in progress.

Table 4. Percentages (avg ± sd**)** of unchanged radiotracer in plasma, brain and liver after radiotracer injection measured using HPLC at different time points and species (**A**: mice; **B**: rats).

A Mice				
		Plasma	Brain	Liver
30 min (n = 3)	[^{18}F]D6-FP-(+)-DTBZ	10.8 ± 3.7	97.1 ± 2.8	19.7 ± 5.5
	[^{18}F]FP-(+)-DTBZ	21.1±7.8	75.7 ± 4.0	21.3 ± 3.2
60 min (n = 5)	[^{18}F]D6-FP-(+)-DTBZ	4.8 ± 1.8	65.6 ± 20.4	9.4 ± 2.0
	[^{18}F]FP-(+)-DTBZ	3.7 ± 2.2	47.5 ± 7.2	8.3 ± 1.3

B Rats				
		Plasma	Brain	Liver
60 min (n = 2)	[^{18}F]D6-FP-(+)-DTBZ	87.5 ± 3.9	94.9 ± 0.4	87.7 ± 2.9
	[^{18}F]FP-(+)-DTBZ	72.9 ± 11.3	94.4 ± 0.6	87.4 ± 0.2

The hydrogen to deuterium substitution presents a clear beneficial effect on improving the in vivo pharmacokinetics of the imaging agents targeting VMAT2 in the brain; as such, the novel new chemical entity with deuterium substitution provides a better specific target binding and regional brain signal for PET imaging of VMAT2 in the brain and an apparent reduction of bone uptake. The hydrogen to deuterium substitution of [^{18}F]FP-(+)-DTBZ to form [^{18}F]D6-FP-(+)-DTBZ suggests reduced rate of in vivo metabolism and improved in vivo pharmacokinetics.

Similar to the recently approved deuterated tetrabenazine, SD-809, the nonradioactive D6-FP-(+)-DTBZ, **1**, which shows a higher binding affinity to the target sites (VMAT2), may also be considered as a useful therapeutic agent for movement disorders.

4. Conclusion

The new VMAT2 imaging agent, [^{18}F]D6-FP-(+)-DTBZ with deuterium substitution provides a good specific target binding and regional brain signal for PET imaging of VMAT2 in the brain. [^{18}F]D6-FP-DTBZ/PET may be useful as a routine clinical tool for diagnosis and monitoring PD patients.

Conflict of interest

Authors declare no conflict of interest.

References:

[1] Meanwell NA. Synopsis of some recent tactical application of bioisosteres in drug design. J. Med. Chem. 2011;54:2529-91.

[2] Guengerich FP. Kinetic deuterium isotope effects in cytochrome P450 oxidation reactions. J Labelled Comp Radiopharm 2013;56:428-31.

[3] Howland RH. Deuterated Drugs. J. Psychosoc. Nurs. Ment. Health Serv. 2015;53:13-6.

[4] Gant TG. Using deuterium in drug discovery: leaving the label in the drug. J. Med. Chem. 2014;57:3595-611.

[5] Jankovic J, Jimenez-Shahed J, Budman C, Coffey B, Murphy T, Shprecher D, et al. Deutetrabenazine in Tics Associated with Tourette Syndrome. Tremor Other Hyperkinet Mov (N Y) 2016;6:422.

[6] Frank S, Testa CM, Stamler D, Kayson E, Davis C, Edmondson MC, et al. Effect of Deutetrabenazine on Chorea Among Patients With Huntington Disease: A Randomized Clinical Trial. JAMA 2016;316:40-50.

[7] Garay RP and Grossberg GT. AVP-786 for the treatment of agitation in dementia of the Alzheimer's type. Expert Opin. Investig. Drugs 2017;26:121-32.

[8] Kuchar M and Mamat C. Methods to Increase the Metabolic Stability of (18)F-Radiotracers. Molecules 2015;20:16186-220.

[9] Fowler JS, Wang GJ, Logan J, Xie S, Volkow ND, MacGregor RR, et al. Selective reduction of radiotracer trapping by deuterium substitution: comparison of carbon-11-L-deprenyl and carbon-11-deprenyl-D_2 for MAO B mapping. J. Nucl. Med. 1995;36:1255-62.

[10] Logan J, Fowler JS, Volkow ND, Wang GJ, MacGregor RR, and Shea C. Reproducibility of repeated measures of deuterium substituted [11C]L-deprenyl ([11C]L-deprenyl-D2) binding in the human brain. Nucl. Med. Biol. 2000;27:43-9.

[11] Eriksson O, Jahan M, Johnstrom P, Korsgren O, Sundin A, Halldin C, et al. In vivo and in vitro characterization of [18F]-FE-(+)-DTBZ as a tracer for beta-cell mass. Nucl. Med. Biol. 2010;37:357-63.

[12] Jahan M, Eriksson O, Johnstrom P, Korsgren O, Sundin A, Johansson L, et al. Decreased defluorination using the novel beta-cell imaging agent [18F]FE-DTBZ-d4 in pigs examined by PET. EJNMMI Res 2011;1:33.

[13] Goswami R, Ponde D, Kung M, Hou C, Kilbourn M, and Kung H. Fluoroalkyl derivatives of dihydrotetrabenazine as positron emission tomography imaging agents targeting vesicular monoamine transporters. Nucl. Med. Biol. 2006;33:685-94.

[14] Kilbourn M, Hockley B, Lee L, Hou C, Goswami R, Ponde D, et al. Pharmacokinetics of [(18)F]fluoroalkyl derivatives of dihydrotetrabenazine in rat and monkey brain. Nucl. Med. Biol. 2007;34:233-7.

[15] Siderowf A, Pontecorvo MJ, Shill HA, Mintun MA, Arora A, Joshi AD, et al. PET imaging of amyloid with Florbetapir F 18 and PET imaging of dopamine degeneration with 18F-AV-133 (florbenazine) in patients with Alzheimer's disease and Lewy body disorders. BMC Neurol. 2014;14:79.

[16] Hsiao IT, Weng YH, Lin WY, Hsieh CJ, Wey SP, Yen TC, et al. Comparison of 99mTc-TRODAT-1 SPECT and 18 F-AV-133 PET imaging in healthy controls and Parkinson's disease patients. Nucl. Med. Biol. 2014;41:322-9.
[17] Hsiao IT, Weng YH, Hsieh CJ, Lin WY, Wey SP, Kung MP, et al. Correlation of Parkinson disease severity and 18F-DTBZ positron emission tomography. JAMA Neurol 2014;71:758-66.
[18] Okamura N, Villemagne V, Drago J, Pejoska S, Dhamija R, Mulligan R, et al. In Vivo Measurement of Vesicular Monoamine Transporter Type 2 Density in Parkinson Disease with 18F-AV-133. J. Nucl. Med. 2010;51:223-8.
[19] Villemagne VL, Okamura N, Pejoska S, Drago J, Mulligan RS, Chetelat G, et al. In vivo assessment of vesicular monoamine transporter type 2 in dementia with lewy bodies and Alzheimer disease. Arch. Neurol. 2011;68:905-12.
[20] Alexander PK, Lie Y, Jones G, Sivaratnam C, Bozinovski S, Mulligan RS, et al. Management Impact of Imaging Brain Vesicular Monoamine Transporter type-2 (VMAT2) in Clinically Uncertain Parkinsonian Syndrome (CUPS) with 18F-AV133 and PET. J. Nucl. Med. 2017.
[21] Harris PE, Farwell MD, and Ichise M. PET quantification of pancreatic VMAT 2 binding using (+) and (-) enantiomers of [(1)(8)F]FP-DTBZ in baboons. Nucl. Med. Biol. 2013;40:60-4.
[22] Normandin MD, Petersen KF, Ding YS, Lin SF, Naik S, Fowles K, et al. In vivo imaging of endogenous pancreatic beta-cell mass in healthy and type 1 diabetic subjects using 18F-fluoropropyl-dihydrotetrabenazine and PET. J. Nucl. Med. 2012;53:908-16.
[23] Chen Z, Tang J, Liu C, Li X, Huang H, Xu X, et al. Effects of anesthetics on vesicular monoamine transporter type 2 binding to (1)(8)F-FP-(+)-DTBZ: a biodistribution study in rat brain. Nucl. Med. Biol. 2016;43:124-9.
[24] Huang CY, Liu CH, Tsao E, Hsieh CJ, Weng YH, Hsiao IT, et al. Chronic manganism: A long-term follow-up study with a new dopamine terminal biomarker of 18F-FP-(+)-DTBZ (18F-AV-133) brain PET scan. J. Neurol. Sci. 2015;353:102-6.
[25] Chang CC, Hsiao IT, Huang SH, Lui CC, Yen TC, Chang WN, et al. (1)(8)F-FP-(+)-DTBZ positron emission tomography detection of monoaminergic deficient network in patients with carbon monoxide related parkinsonism. Eur. J. Neurol. 2015;22:845-52, e59-60.
[26] de la Fuente-Fernandez R, Schulzer M, Kuramoto L, Cragg J, Ramachandiran N, Au WL, et al. Age-specific progression of nigrostriatal dysfunction in Parkinson's disease. Ann. Neurol. 2011;69:803-10.
[27] Kung M, Hou C, Goswami R, Ponde D, Kilbourn M, and Kung H. Characterization of optically resolved 9-fluoropropyl-dihydrotetrabenazine as a potential PET Imaging agent targeting vesicular monoamine transporters. Nucl. Med. Biol. 2007;34:239-46.